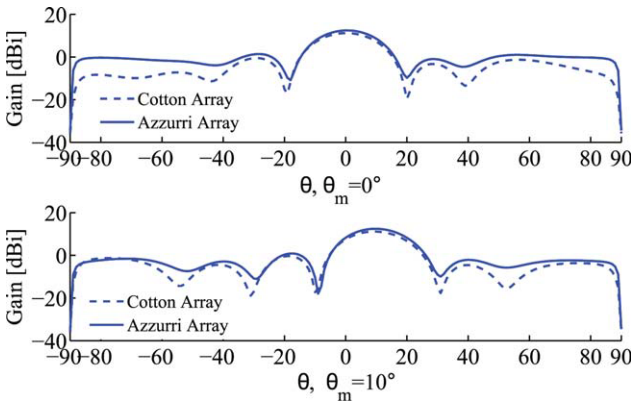

Figure 4 Gain pattern at 2.45 GHz of the antenna array in the *xz*-plane, steering the beam along $\theta_m = 0°$ and 10°. [Color figure can be viewed in the online issue, which is available at wileyonlinelibrary.com]

humidity conditions were presented. The array is intended to provide more reliable off-body communication links within the 2.45 GHz ISM band and to be worn by rescue workers or fire fighters, active in a disaster area. Compared to a nonuniform array, the ULA guarantees low mutual coupling between the radiating elements, a narrow main beam, low side lobes, and relatively easy steering. In general, when choosing a textile material as a substrate for a textile antenna array to integrate into a garment, the MR value of the textile material must be taken into account. Here, it was shown, under reproducible rH conditions realized in a climate test cabinet, that the array on Azzurri foam exhibits perfectly stable reflection coefficient characteristics of each individual antenna element. For the implementation on cotton, however, the resonance frequency decreases with increasing rH, and the ISM band is no longer covered, when the rH is above 70%. Thanks to the ETMPA topology of the individual patches, the relatively small number of radiating elements, and the rather large spacing of $3/4\lambda$ between them, the mutual coupling is always low, even for the implementation on cotton, where the influence of rH is again noticeable. Hence, a low-cost array design with a large antenna aperture of about 50 cm and with limited steering capabilities centered around the broadside direction is obtained. When limiting the steering angle to 10° around the broadside direction, no grating lobes appear.

REFERENCES

1. M. Klemm, I. Locher, and G. Tröster, A novel circularly polarized textile antenna for wearable applications, In: Proc. of 7th European microwave week, 2004, pp. 137–140.
2. P. Salonen and H. Hurme, A novel fabric WLAN antenna for wearable applications, In: IEEE antennas and propagation society international symposium, Columbus, OH, 2003, pp. 700–703.
3. C. Hertleer, A. Tronquo, H. Rogier, and L. Van Langenhove, The use of textile materials to design wearable microstrip patch antennas, Textile Res J 78 (2008), 651–658.
4. C. Hertleer, H. Rogier, and L. Van Langenhove, A textile antenna for protective clothing, In: 2007 IET seminar on antennas and propagation for body-centric wireless communications, 2007, pp. 44–46.
5. C. Hertleer, A. Van Laere, H. Rogier, and L. Van Langenhove, Influence of relative humidity on textile antenna performance, Textile Res J 80 (2010), 177–183.
6. S. Sadat Karimabadi, Y. Mohsenzadeh, A. Reza Attari, and S. Mahdi Moghadasi, Bandwidth enhancement of single-feed circularly polarized equilateral triangular microstrip antenna, In: Progress in electromagnetic research symposium, Hangzhou, China, 2008, pp. 147–150.
7. C. Tang, J. Lu, and K. Wong, Circularly polarized equilateral-triangular microstrip antenna with truncated tip, Electron Lett 34 (1998), 1277–1278.
8. F. Declercq, I. Couckuyt, H. Rogier, and T. Dhaene, Complex permittivity characterization of textile materials by means of surrogate modelling, In: IEEE international symposium on antennas and propagation and CNC-USNC/URSI radio science meeting, July 2010.

WWAN/LTE PRINTED SLOT ANTENNA FOR TABLET COMPUTER APPLICATION

Kin-Lu Wong and Wun-Jian Lin
Department of Electrical Engineering, National Sun Yat-Sen University, Kaohsiung 804, Taiwan, Republic of China;
Corresponding author: wongkl@ema.ee.nsysu.edu.tw

Received 17 March 2011

ABSTRACT: *A printed slot antenna comprising two quarter-wavelength slots of different lengths and a half-wavelength slot for eight-band wireless wide area network/long term evolution operation in the tablet computer is presented. The two quarter-wavelength slots are open slots or monopole slots, and the half-wavelength slot is aligned in-between the two quarter-wavelength slots. The three slots are excited using a two-strip feedline which is printed on the opposite surface of the printed slots. The proposed three-slot configuration can lead to two wide operating bands, with the lower one covering the 704–960 MHz band and the upper one covering the 1710–2690 MHz band. Good radiation efficiency for frequencies over the operating bands is obtained. The simulated body specific absorption rate values of the antenna in the bottom face, landscape and portrait orientations to the flat phantom in the body specific absorption rate testing model also meet the limit of 1.6 W/kg for 1-g tissue. Details of the results are presented.* © 2011 Wiley Periodicals, Inc. Microwave Opt Technol Lett 54:44–49, 2012; View this article online at wileyonlinelibrary.com. DOI 10.1002/mop.26509

Key words: *mobile antennas; internal tablet computer antennas; printed slot antennas; WWAN antennas; LTE antennas; body SAR*

1. INTRODUCTION

Printed slot antennas are easy to fabricate at low cost and have been shown to be promising for applications in the mobile devices such as handsets and laptop computers as internal wireless wide area network (WWAN) antennas [1–11]. These printed slot antennas include the use of the traditional half-wavelength slots with two closed ends [2, 4] and the quarter-wavelength slots or monopole slots with one open end and one closed end [1, 3–11]. To achieve compact antenna size and multiband or wideband operation such as the penta-band WWAN operation (GSM850/900/1800/1900/UMTS), the use of two or three slot elements have been applied. It has also been noted that when there is more than one slot, the relative alignment of the slots is important in achieving wideband operation with a compact antenna size. For example, for the reported internal WWAN slot antennas for laptop computer applications, promising two-slot and three-slot configurations have been demonstrated [9, 10]. For the two-slot case, the design using two monopole slots with their open ends disposed at opposite edges has been reported [10], in which a T-shaped feedline is used to feed the two slots. For the three-slot case, the design using three monopole slots with their open ends disposed at the same edge and their closed ends extended in about the same direction has been demonstrated [9], and a step-shaped feedline is used to feed the three slots. For

these two cases [9, 10], two wide operating bands can be obtained to cover the GSM850/900 operation (824–960 MHz) and the GSM1800/1900/UMTS operation (1710–2170 MHz). With these reported slot configurations, however, further enhancement in their operating bandwidth is difficult to obtain, especially for their lower-band bandwidth to cover the additional LTE700 operation (704–787 MHz).

The long term evolution (LTE) operation, which is recently introduced to provide much higher data rate than the WWAN operation, mainly includes three operating bands in the LTE700, LTE2300 (2300–2400 MHz), and LTE2500 (2500–2690 MHz) and is becoming demanded for the modern mobile devices [12–15]. However, it is noted that there are still no slot antennas reported in the published papers capable of covering both the WWAN and LTE operations, that is, eight-band WWAN/LTE operation in the 704–960 and 1710–2690 MHz bands.

In this article, we present a new three-slot configuration with a compact antenna size to cover eight-band WWAN/LTE operation in the tablet computer. The three slots include two monopole slots of different lengths and a traditional half-wavelength slot aligned in-between the two monopole slots. Since the excited electric fields near the closed end of the half-wavelength slot are generally very weak, different from those excited near the open ends of the two monopole slots which are generally the strongest inside the monopole slot [16–21], the proposed slot configuration can hence lead to small coupling between the three slots. This makes it very promising to achieve a compact three-slot configuration for decreased antenna size yet wideband or multiband operation to cover the desired 704–960 and 1710–2690 MHz bands. In addition, to efficiently excite the three slots, a two-branch feedline is applied. Details of the design considerations of the proposed antenna are presented in the article.

Also note that, the tablet computer in the study is of one-section slate type and is different from the traditional laptop computers with a foldable two-section structure [10, 22–24]. The internal antennas in the tablet computers are generally mounted along the perimeter of the display and are hence with a small distance of much less than 20 mm to the user's body in practical applications. This condition makes the tablet computer antenna not only required to cover the desired multiband operation, but also demanded to be tested for the body specific absorption rate (SAR) [25]. To be accepted for practical applications, the body SAR for 1-g body tissue should be less than 1.6 W/kg [26, 27]. To meet this practical requirement, the simulated body SAR results of the proposed antenna are presented.

2. PROPOSED THREE-SLOT ANTENNA

Figure 1 shows the geometry of the proposed slot antenna for tablet computer application. The antenna comprises two monopole slots (slot 1 and slot 2) and one half-wavelength slot (slot 3). The antenna is mounted along the front edge of the shielding metal wall (length 200 mm, width 5 mm) of the display ground in the tablet computer. In addition, the antenna is placed close to one corner of the shielding wall with a distance of 15 mm such that more possible internal antennas can be accommodated along the shielding wall. In the study, the tablet computer with a 9.7-inch display is considered, which is presently available in the market. The dimensions of the display ground are hence selected to be 200 × 150 mm^2, which supports a 9.7-inch display. The display is also assumed to have a thickness of 5 mm and is disposed at the front side of the tablet computer.

Note that the tablet computer housing is not included in the study. However, to simulate a practical housing in the body

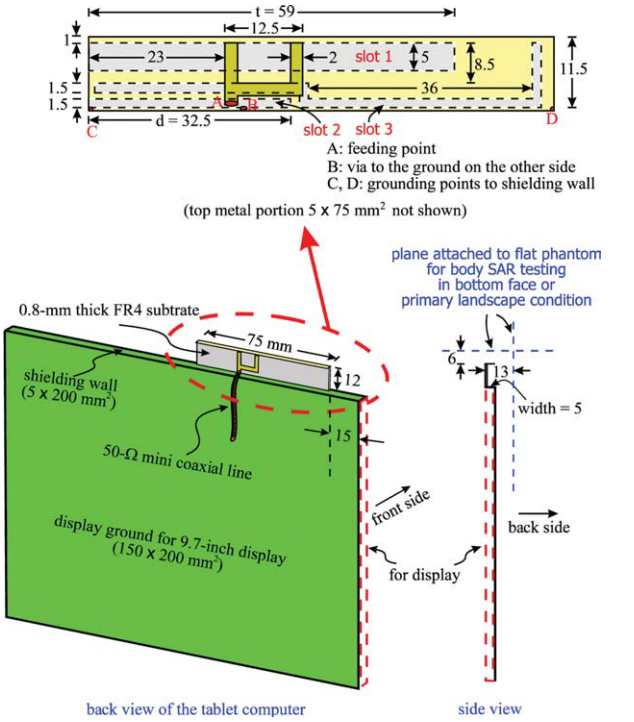

Figure 1 Geometry of the WWAN/LTE printed slot antenna for tablet computer application. [Color figure can be viewed in the online issue, which is available at wileyonlinelibrary.com]

SAR testing [25], the antenna is assumed to be positioned at a distance of 13 mm to the flat phantom in the bottom face condition. While for the primary landscape condition, the distance between the antenna and the flat phantom is set to 6 mm. Detailed orientations of the antenna with respect to the flat phantom in different body SAR testing conditions will be discussed in Section 3 with the aid of Figure 11.

The antenna is mainly printed on a 0.8-mm thick FR4 substrate of relative permittivity 4.4, loss tangent 0.02, and size 75 × 12 mm^2. A top metal portion of size 5 × 75 mm^2 is added for improving the impedance matching of the antenna, especially for improving the impedance matching of the frequencies in the antenna's lower band. The top metal portion is oriented orthogonal to the FR4 substrate and parallel to the shielding metal wall. Slot 1 has a width of 5 mm and its length (t) is elected to be 59 mm. Slot 1 (a monopole slot) can contribute a 0.25-wavelength slot resonant mode at about 900 MHz, which alone however cannot cover the desired 704–960 MHz band. With the presence of slot 3 (a traditional slot) which has a width of 1.5 mm and a length of about 82 mm, a 0.5-wavlength slot resonant mode at about 0.75 GHz can be generated to greatly enhance the lower-band bandwidth of the antenna such that the LTE700/GSM850/900 operation in the 704–960 MHz band is covered.

Slot 2 (a monopole slot) with a width of 1.5 mm and a length (d) of 32.5 mm can contribute a 0.25-wavelength slot resonant mode at about 1.7 GHz to combine with the higher-order resonant modes contributed by slot 1 and slot 3 respectively at about 2.8 and 2.4 GHz to form the antenna's upper band. The upper band can have a wide bandwidth of larger than 1 GHz to cover the GSM1800/1900/UMTS/LTE2300/2500 operation in the 1710–2690 MHz band.

To successfully excite the three slots, a novel two-branch feedline is applied, which comprises a main feeding strip and a branch feeding strip. The main feeding strip passes through the

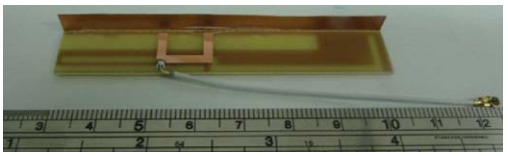

Figure 2 Photo of the fabricated antenna. [Color figure can be viewed in the online issue, which is available at wileyonlinelibrary.com]

three slots, while the branch feeding strip passes slot 1 and slot 3 only. The branch feeding strip can greatly enhance the impedance matching of the excited slot resonant modes of the antenna, and lead to two wide operating bands for covering the desired 704–960 and 1710–2690 MHz bands. Detailed effects of the branch feeding strip are discussed in Section 3 with the aid of Figure 6.

The front end (point A) of the two-branch feedline is the antenna's feeding point, which is connected to the central conductor of a 50-Ω mini coaxial line as shown in the figure to test the antenna in the experiment. The grounding sheath of the mini coaxial line is connected through a via-hole at point B to the ground plane on the other side of the FR4 substrate. A photo of the fabricated antenna with a mini coaxial line is shown in Figure 2. Note that there is a metal potion (a 0.2-mm copper plate in the experiment) of size 5×75 mm^2 added at the top edge of the antenna to enhance the impedance matching of the antenna. In the experiment, the ground plane of the antenna is grounded to the shielding metal wall at point C and D. Measured results and parametric study of the proposed antenna are presented in Section 3.

3. RESULTS AND DISCUSSION

Figure 3 shows the measured and simulated return loss of the antenna. The simulated results are obtained using the full-wave electromagnetic field simulation software HFSS version 12 [28]. The simulated results agree with the measured data. Two wide operating bands are obtained. Over the desired 704–960 and 1710–2690 MHz bands, the impedance matching is better than 6-dB return loss (3:1 VSWR), which is the widely used design specification of the internal WWAN and LTE antennas for mobile devices.

Figure 4 shows the measured antenna efficiency (mismatching loss included) of the antenna. The antenna with the display ground shown in Figure 1 is tested in a far-field anechoic chamber. Good antenna efficiency (all better than 50% over the operating bands) is obtained for the antenna. The antenna efficiency is in the range of about 56–72% and 60–75% for frequencies in

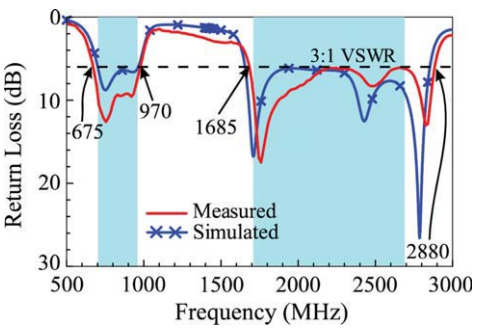

Figure 3 Measured and simulated return loss of the antenna. [Color figure can be viewed in the online issue, which is available at wileyonlinelibrary.com]

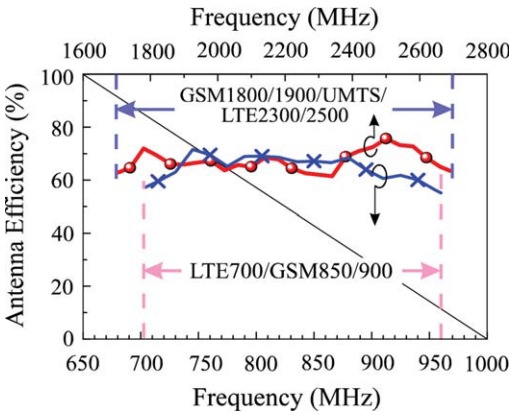

Figure 4 Measured antenna efficiency (mismatching loss included) of the antenna. [Color figure can be viewed in the online issue, which is available at wileyonlinelibrary.com]

the lower and upper bands, respectively. The measured three-dimensional total-power radiation patterns at typical frequencies are plotted in Figure 5. At lower frequencies of 740 and 925 MHz, some differences in the radiation patterns are seen. This is largely because the two frequencies are related to different resonant modes, one being the 0.5-wavelength mode of slot 3 and the other being the 0.25-wavelength mode of slot 1. Also, the radiation patterns at the two lower frequencies are different from the dipole-like patterns commonly seen for the internal handset antennas [29, 30]. This behavior is in part because the large display ground is no longer an efficient radiator in this study, different from the handset chassis usually as efficient

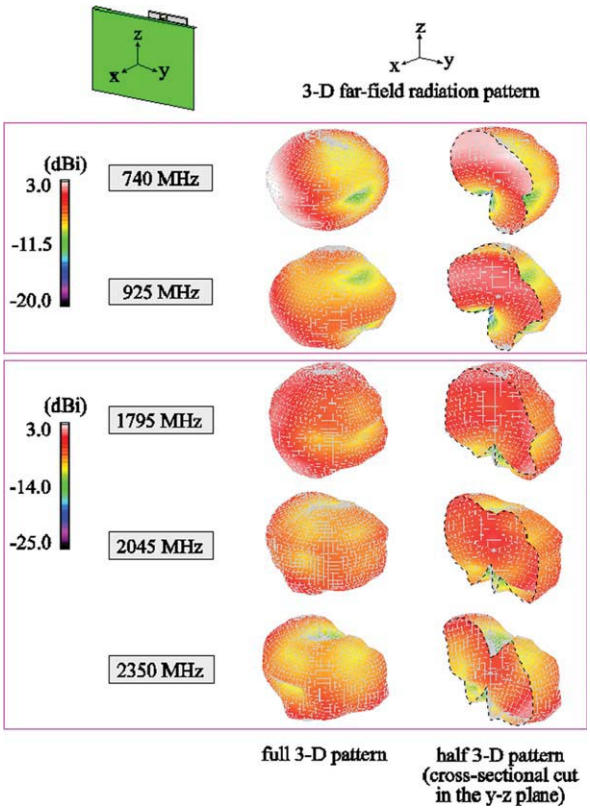

Figure 5 Measured three-dimensional radiation patterns of the antenna. [Color figure can be viewed in the online issue, which is available at wileyonlinelibrary.com]

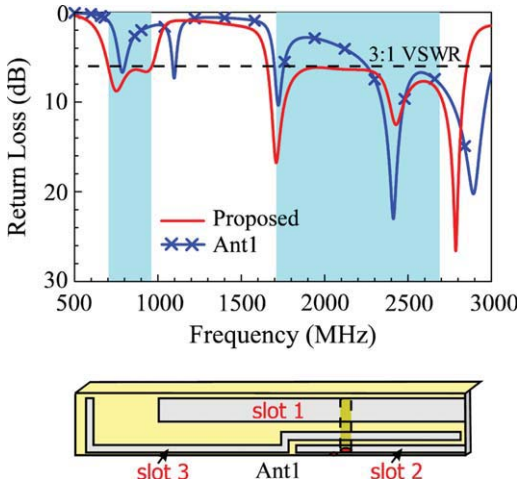

Figure 6 Simulated return loss for the proposed antenna and the case without the branch feeding strip (Ant1). [Color figure can be viewed in the online issue, which is available at wileyonlinelibrary.com]

radiators [31], and in addition, the proposed antenna is asymmetrically mounted along the front edge of the top shielding wall of the display ground. The latter will cause some asymmetric in the radiation patterns. At higher frequencies of 1795, 2045, and 2350 MHz, variations in the radiation patterns are also seen. This behavior is related to the different resonant modes (higher-order resonant modes of slot 1 and slot 3) excited to form the antenna's upper band.

To further analyze the operating principle of the antenna, Figure 6 shows the simulated return loss for the proposed antenna and the case with the main feeding strip only (Ant1). Corresponding dimensions of the two antennas are the same. Results show that although all the desired slot resonant modes contributed by the three slots in this study can be excited by the main feeding strip alone, good impedance matching of some excited resonant modes cannot be obtained, especially the two modes contributed by slot 1 and slot 3 for the antenna's lower band. By adding the branch feeding strip, which passes through slot 1 and slot 3 at additional feeding positions, good impedance matching of all the desired slot resonant modes can be obtained, and two wide operating band for covering eight-band WWAN/LTE operation are achieved.

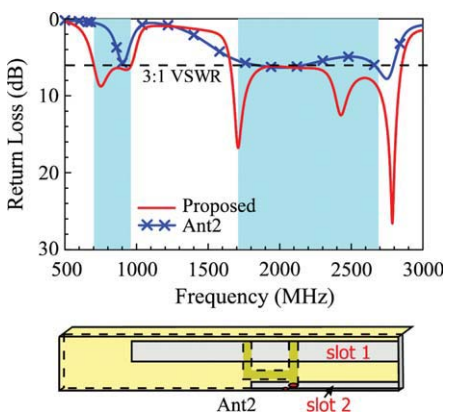

Figure 7 Simulated return loss for the proposed antenna and the case without slot 3 (Ant2). [Color figure can be viewed in the online issue, which is available at wileyonlinelibrary.com]

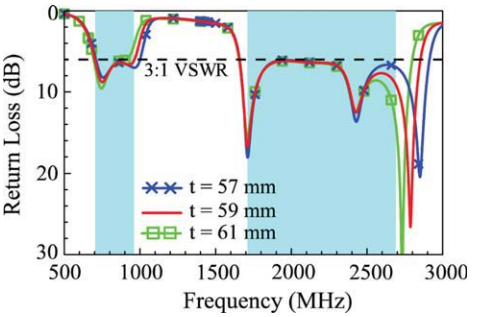

Figure 8 Simulated return loss as a function of the length t of slot 1. Other dimensions are the same as in Fig. 1. [Color figure can be viewed in the online issue, which is available at wileyonlinelibrary.com]

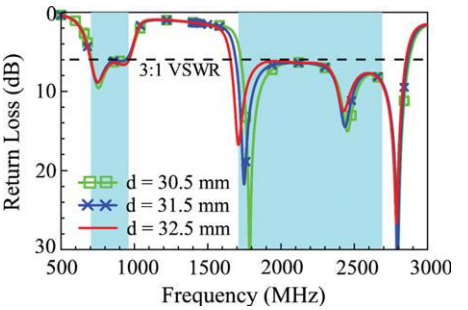

Figure 9 Simulated return loss as a function of the length d of slot 2. Other dimensions are the same as in Fig. 1. [Color figure can be viewed in the online issue, which is available at wileyonlinelibrary.com]

Figure 7 shows the simulated return loss for the proposed antenna and the case without slot 3 (Ant2). For the antenna's lower band, it is seen that only one resonant mode at about 0.9 GHz is excited, which is contributed mainly by slot 1. With the presence of slot 3 disposed in-between slot 1 and slot 2, additional resonant modes at about 0.7 GHz for widening the antenna's lower-band bandwidth and at about 2.4 GHz for widening the upper-band bandwidth are generated. In addition, the presence of slot 3 also leads to good excitation of the resonant modes contributed by slot 2 at about 1.7 GHz and by slot 1 at about 2.8 GHz. This behavior is mainly because the disposition of slot 3 (a traditional slot) in-between slot 1 and slot 2 (monopole slots) can lead to small coupling between the three slots, thus making it possible to achieve a compact antenna size yet wideband or multiband operation to cover the desired 704–960 and 1710–2690 MHz bands.

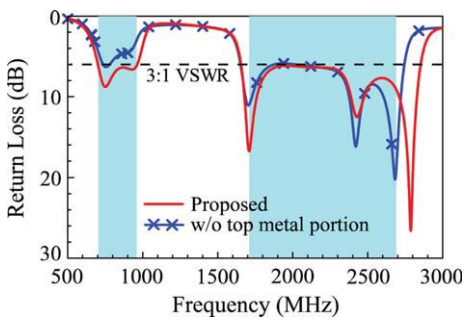

Figure 10 Simulated return loss for the proposed antenna and the case without the top metal portion. [Color figure can be viewed in the online issue, which is available at wileyonlinelibrary.com]

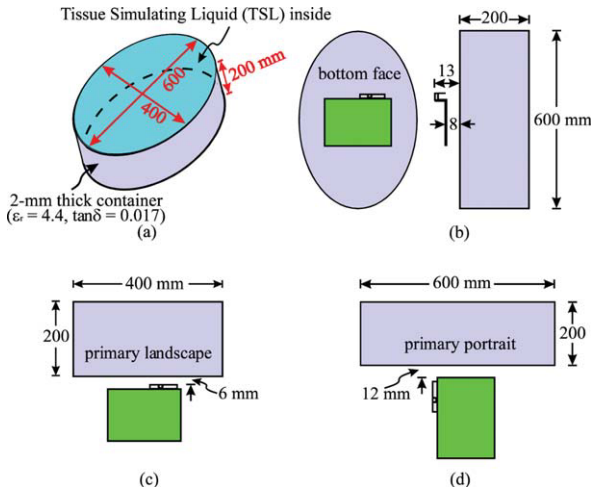

Figure 11 Body SAR simulation models. (a) Flat phantom. (b) Bottom face condition (top view). (c) Primary landscape condition. (d) Primary portrait condition. [Color figure can be viewed in the online issue, which is available at wileyonlinelibrary.com]

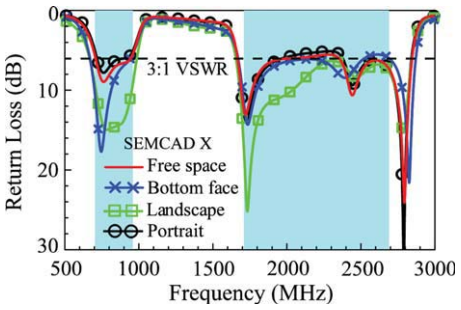

Figure 12 Simulated return loss for the antenna in free space and the antenna with the flat phantom in the bottom face, primary landscape, and primary portrait conditions. [Color figure can be viewed in the online issue, which is available at wileyonlinelibrary.com]

A parametric study of some design dimensions is also conducted. Figure 8 shows the simulated return loss as a function of the length t of slot 1. Other dimensions are the same as in Figure 1. Results for the length t varied from 57 to 61 mm are shown. Results show that the resonant modes at about 0.9 and 2.8 GHz are shifted to higher frequencies with a decrease in the length t, which confirms that these two resonant modes are mainly contributed by slot 1. For other resonant modes, there are very small effects observed. This feature makes it easy to control or adjust the excited resonant modes of the antenna.

Figure 9 shows the simulated return loss as a function of the length d of slot 2, with other dimensions the same as in Figure 1. Results for the length d varied from 30.5 to 32.5 mm are shown. It is seen that the resonant mode at about 1.7 GHz is shifted to higher frequencies with a decrease in the length d. This feature also confirms that this resonant mode is mainly contributed by slot 2. Again, very small effects on the impedance matching of other resonant modes are seen. This also makes it easy to adjust the excited resonant modes of the antenna.

Figure 10 shows the simulated return loss for the proposed antenna and the case without the top metal portion. Large effects are seen on the two resonant modes in the lower band and on the resonant mode at about 2.8 GHz in the upper band. This behavior is largely because without the top metal portion, slot 1 will have no sufficient surrounding ground plane size for lower-frequency operation, thus making it difficult to excite the slot resonant mode at about 900 MHz. This also affects good excitation of the slot resonant mode at about 0.7 GHz contributed by slot 3. As for the resonant mode at about 2.8 GHz contributed by slot 1, it is interesting to see that it is shifted to lower frequencies when the top metal portion is not present. The result suggests that a sufficient surrounding ground plane size is important for good excitation of the slot antenna.

The body SAR [25] is then tested for the antenna to meet the requirements for practical applications. Figure 11 shows the body SAR simulation model for the antenna based on the simulation software SEMCAD X version 14 [32]. In the simulation model, a flat phantom shown in Figure 11(a) is used to simulate the human body. The flat phantom is formed by filling a plastic elliptic cylindrical container with tissue simulating liquid [33]. The dimensions of the flat phantom are shown in the figure. Although there are five testing conditions of the bottom face [see Fig. 11(b)], primary landscape [Fig. 11(c)], primary portrait [Fig. 11(d)], secondary landscape, and secondary portrait in the body SAR regulation [25], the last two conditions in which the antenna has a large distance (>100 mm) to the flat phantom and will have a very small SAR values (usually less than 0.1 W/kg for 1-g tissue) are not tested in this study. Note that the practical tablet computer housing is not included in the test. The length 13 mm shown in Figure 11(b) for the bottom face condition indicates the width of the promising tablet computer housing, while the length 6 mm in Figure 11(c) for the primary landscape condition shows the distance between the top surface of the housing and the top edge of the antenna, and the length 12 mm shows the distance between the side edge of the display ground and the side surface of the housing which is attached to the flat phantom.

Results of the simulated return loss obtained using SEMCAD X [32] for the antenna in free space and the antenna with the flat phantom in the bottom face, primary landscape, and primary portrait conditions are first presented in Figure 12. For the antenna in free space, it is seen that the simulated results using SEMCAD X are similar to those shown in Figure 3 using HFSS. Some variations in the return loss are seen which is

TABLE 1 Simulated Body SAR Results Obtained Using SEMCAD X [32] for 1 g Tissue

Frequency (MHz)		740	859	925	1795	1920	2045	2350	2595
Input power (Watt)		0.125	0.25	0.25	0.125	0.125	0.125	0.125	0.125
1-g SAR (W/kg)	Bottom face	0.53	0.97	1.07	1.18	0.73	0.62	0.62	0.97
	Primary landscape	0.36	0.94	1.36	1.23	0.69	0.52	0.57	1.37
	Primary portrait	0.25	0.23	0.07	0.06	0.05	0.07	0.04	0.12
Return loss (dB)	Bottom face	17.2	7.8	6.5	10.6	7.2	6.5	8.0	5.6
	Primary landscape	13.0	14.5	12.6	14.7	11.4	10.0	6.8	7.0
	Primary portrait	6.1	5.9	9.4	6.6	5.9	5.8	6.5	7.0
Free space	8.2	6.9	6.4	8.7	6.4	6.2	6.2	6.3	

The return loss shows the impedance matching level of the antenna at each testing frequency.

owing to the presence of the flat phantom. The obtained SAR results for 1-g body tissue at the central frequencies of the eight operating bands are shown in Table 1. The input power at each frequency is 0.25 Watt (24 dBm) at 859 and 925 MHz for GSM850/900 operation and 0.125 Watt (21 dBm) at 1795, 1920, 2045, 740, 2350, and 2595 MHz for GSM1800/1900, UMTS and LTE operation. The SAR results all less than the limit of 1.6 W/kg for the three conditions. It is also seen that the SAR results for the primary portrait condition are all less than about 0.25 W/kg and are the smallest among the three body SAR conditions for the eight testing frequencies. This behavior is reasonable since the antenna in the primary portrait condition has the largest distance to the flat phantom among the three conditions.

4. CONCLUSION

A promising three-slot antenna suitable for tablet computer applications to cover eight-band WWAN/LTE operation has been proposed. A two-strip feedline for exciting the three-slot antenna has also been introduced. Detailed operating principle and parametric study of the three-slot antenna has been discussed. The antenna shows good radiation efficiency for frequencies over the eight operating bands. Acceptable body SAR values for 1-g tissue for the antenna applied in the tablet computer have also been obtained, suggesting that the proposed antenna is promising for practical applications.

REFERENCES

1. P. Lindberg, E. Ojefors, and A. Rydberg, Wideband slot antenna for low-profile hand-held terminal applications, Proc 36th European Microwave Conf (EuMC2006), Manchester, UK, 2006, pp. 1698–1701.
2. K.L. Wong, Y.W. Chi, and S.Y. Tu, Internal multiband printed folded slot antenna for mobile phone application, Microwave Opt Technol Lett 49 (2007), 1833–1837.
3. C.I. Lin and K.L. Wong, Printed monopole slot antenna for internal multiband mobile phone antenna, IEEE Trans Antennas Propag 55 (2007), 3690–3697.
4. C.H. Wu and K.L. Wong, Hexa-band internal printed slot antenna for mobile phone application, Microwave Opt Technol Lett 50 (2008), 35–38.
5. C.H. Wu and K.L. Wong, Internal hybrid loop/monopole slot antenna for quad-band operation in the mobile phone, Microwave Opt Technol Lett 50 (2008), 795–801.
6. C.H. Chang and K.L. Wong, Internal multiband surface-mount monopole slot chip antenna for mobile phone application, Microwave Opt Technol Lett 50 (2008), 1273–1279.
7. C.I. Lin and K.L. Wong, Printed monopole slot antenna for penta-band operation in the folder-type mobile phone, Microwave Opt Technol Lett 50 (2008), 2237–2241.
8. F.H. Chu and K.L. Wong, Simple folded monopole slot antenna for penta-band clamshell mobile phone application, IEEE Trans Antennas Propag 57 (2009), 3680–3684.
9. K.L. Wong and L.C. Lee, Multiband printed monopole slot antenna for WWAN operation in the laptop computer, IEEE Trans Antennas Propag 57 (2009), 324–330.
10. K.L. Wong and F.H. Chu, Internal planar WWAN laptop computer antenna using monopole slot elements, Microwave Opt Technol Lett 51 (2009), 1274–1279.
11. K.L. Wong, W.J. Chen, L.C. Chou, and M.R. Hsu, Bandwidth enhancement of the small-size internal laptop computer antenna using a parasitic open slot for the penta-band WWAN operation, IEEE Trans Antennas Propag 58 (2010), 3431–3435.
12. C.T. Lee and K.L. Wong, Planar monopole with a coupling feed and an inductive shorting strip for LTE/GSM/UMTS operation in the mobile phone, IEEE Trans Antennas Propag 58 (2010), 2479–2483.
13. F.H. Chu and K.L. Wong, Simple planar printed strip monopole with a closely-coupled parasitic shorted strip for eight-band LTE/GSM/UMTS mobile phone, IEEE Trans Antennas Propag 58 (2010), 3426–3431.
14. K.L. Wong, W.Y. Chen, C.Y. Wu, and W.Y. Li, Small-size internal eight-band LTE/WWAN mobile phone antenna with internal distributed LC matching circuit, Microwave Opt Technol Lett 52 (2010), 2244–2250.
15. S.C. Chen and K.L. Wong, Bandwidth enhancement of coupled-fed on-board printed PIFA using bypass radiating strip for eight-band LTE/GSM/UMTS slim mobile phone, Microwave Opt Technol Lett 52 (2010), 2059–2065.
16. S.K. Sharma, L. Shafai and N. Jacob, Investigation of wide-band microstrip slot antenna, IEEE Trans Antennas Propag 52 (2004), 865–872.
17. A.P. Zhao and J. Rahola, Quarter-wavelength wideband slot antenna for 3–5 GHz mobile applications, IEEE Antennas Wireless Propag Lett 4 (2005), 421–424.
18. W.S. Chen and K.Y. Ku, Band-rejected design of the printed open slot antenna for WLAN/WiMAX operation, IEEE Trans Antennas Propag 56 (2008), 1163–1169.
19. W.S. Chen and K.Y. Ku, Broadband design of a small non-symmetric ground $\lambda/4$ open slot antenna, Microwave J 50 (2007), 110–120.
20. R. Bancroft, Dual slot radiator single feedpoint printed circuit board antenna, U.S. Pat. 7,129,902, 2006.
21. H. Wang, M. Zheng, and S.Q. Zhang, Monopole slot antenna, U.S. Pat. 6,618,020, 2003.
22. G.H. Huff, J. Feng, S. Zhang, G. Cung, and J.T. Bernhard, Directional reconfigurable antennas on laptop computers: Simulation, measurement and evaluation of candidate integration positions, IEEE Trans Antennas Propag 52 (2004), 3220–3227.
23. K.L. Wong and P.J. Ma, Coupled-fed loop antenna with branch radiators for internal LTE/WWAN laptop computer antenna, Microwave Opt Technol Lett 52 (2010), 2662–2667.
24. T.W. Kang, K.L. Wong, L.C. Chou, and M.R. Hsu, Coupled-fed shorted monopole with a radiating feed structure for eight-band LTE/WWAN operation in the laptop computer, IEEE Trans Antennas Propag 59 (2011), 674–679.
25. Federal Communications Commission, Office of Engineering and Technology, Mobile and Portable Device RF Exposure Equipment Authorization Procedures, OET/Lab Knowledge Database publication number 447498 item 7, December 13, 2007.
26. American National Standards Institute (ANSI), Safety levels with respect to human exposure to radio frequency electromagnetic fields, 3 kHz to 300 GHz, ANSI/IEEE standard C95.1, April 1999.
27. IEC 62209–1, Human exposure to radio frequency fields from hand-held and body-mounted wireless communication devices—Human models, instrumentation, and procedures—Part 1: Procedure to determine the specific absorption rate (SAR) for hand-held devices used in close proximity to the ear (frequency range of 300 MHz to 3 GHz), February 2005.
28. http://www.ansys.com/products/hf/hfss/, ANSYS HFSS.
29. K.L. Wong, Planar antennas for wireless communications, Wiley, New York, 2003.
30. K.L. Wong, W.Y. Chen, and T.W. Kang, On-board printed coupled-fed loop antenna in close proximity to the surrounding ground plane for penta-band WWAN mobile phone, IEEE Trans Antennas Propag 59 (2011), 751–757.
31. Y.W. Chi and K.L. Wong, Compact multiband folded loop chip antenna for small-size mobile phone, IEEE Trans Antennas Propag 56 (2008), 3797–3803.
32. http://www.semcad.com, SPEAG SEMCAD, Schmid & Partner Engineering AG.
33. http://www.ntt-at.com/products_e/sar/index.html, Tissue Simulating Liquid for SAR Measurement, NTT Advanced Technology Corporation.